The Plant Cell, Vol. 13, 1511–1525, July 2001, www.plantcell.org © 2001 American Society of Plant Biologists

RESEARCH ARTICLE

A New Dynamin-Like Protein, ADL6, Is Involved in Trafficking from the *trans*-Golgi Network to the Central Vacuole in Arabidopsis

Jing Bo Jin,[a] Young A Kim,[b] Soo Jin Kim,[b] Sung Hoon Lee,[b] Dae Heon Kim,[b] Gang-Won Cheong,[c] and Inhwan Hwang[b,1]

[a] Department of Molecular Biology, Gyeongsang National University, Chinju 660-701, Korea
[b] Center for Plant Intracellular Trafficking and Division of Molecular and Life Sciences, Pohang University of Science and Technology, Pohang 790-784, Korea
[c] Department of Biochemistry, Gyeongsang National University, Chinju 660-701, Korea

Dynamin, a high-molecular-weight GTPase, plays a critical role in vesicle formation at the plasma membrane during endocytosis in animal cells. Here we report the identification of a new dynamin homolog in Arabidopsis named Arabidopsis dynamin-like 6 (ADL6). ADL6 is quite similar to dynamin I in its structural organization: a conserved GTPase domain at the N terminus, a pleckstrin homology domain at the center, and a Pro-rich motif at the C terminus. In the cell, a majority of ADL6 is associated with membranes. Immunohistochemistry and in vivo targeting experiments revealed that ADL6 is localized to the Golgi apparatus. Expression of the dominant negative mutant ADL6[K51E] in Arabidopsis protoplasts inhibited trafficking of cargo proteins destined for the lytic vacuole and caused them to accumulate at the *trans*-Golgi network. In contrast, expression of ADL6[K51E] did not affect trafficking of a cargo protein, H^+-ATPase:green fluorescent protein, destined for the plasma membrane. These results suggest that ADL6 is involved in vesicle formation for vacuolar trafficking at the *trans*-Golgi network but not for trafficking to the plasma membrane in plant cells.

INTRODUCTION

In eukaryotic cells, a large number of proteins are transported to their final destination by a process called intracellular trafficking. During the past two decades, intracellular trafficking has been studied extensively in yeast, animal, and plant cells (Rothman, 1994; Hawes et al., 1999; Jahn and Südhof, 1999; Bassham and Raikhel, 2000). As in the cases of animal and yeast cells, the endoplasmic reticulum (ER), Golgi apparatus, plasma membrane, and vacuoles are the main components of the endomembrane systems in plant cells, and it is generally assumed that the mechanism of intracellular trafficking between compartments in plant cells would be similar to that in other systems (Hawes et al., 1999). Recent advances in the understanding of intracellular trafficking in plant cells support this notion. For example, many plant genes have been shown to complement mutations in corresponding genes in yeast cells (Bassham et al., 1995; Takeuchi et al., 1998). Furthermore, many proteins known to be involved in trafficking, such as clathrin, the coatomer subunits of coat protein 1 (COPI) vesicles, various soluble *N*-ethylmaleimide–sensitive factor attachment protein receptors, and many small GTP binding proteins, have been identified in plant cells (Lebas and Axelos, 1994; Blackbourn and Jackson, 1996; Movafeghi et al., 1999; Pimpl et al., 2000; Sanderfoot et al., 2000; Takeuchi et al., 2000).

AtVPS45, a homolog of yeast Sec1p that is thought to be involved in vesicle fusion, has been identified in Arabidopsis (Bassham et al., 2000), and Kim et al. (2001) recently demonstrated that phosphatidylinositol 3-phosphate [PI(3)P] plays an important role in vacuolar trafficking in plant cells, as it does in animal and yeast cells (Schu et al., 1993; Jones and Howell, 1997). However, recent studies also have revealed many differences between plant and animal cells in intracellular trafficking (Baba et al., 1997; Bassham and Raikhel, 2000; Toyooka et al., 2000). An example of this is the presence in plant cells of at least two different types of vacuoles: lytic and storage vacuoles (Neuhaus and Rogers, 1998). The lytic vacuole is thought to be similar to the vacuole of yeast cells or the lysosome of animal cells, whereas an organelle that is similar to the plant storage vacuole is not present in yeast or animal cells, suggesting that trafficking between the storage vacuole and other organelles is likely unique to plant cells

[1] To whom correspondence should be addressed. E-mail ihhwang@postech.ac.kr; fax 82-54-279-8159.

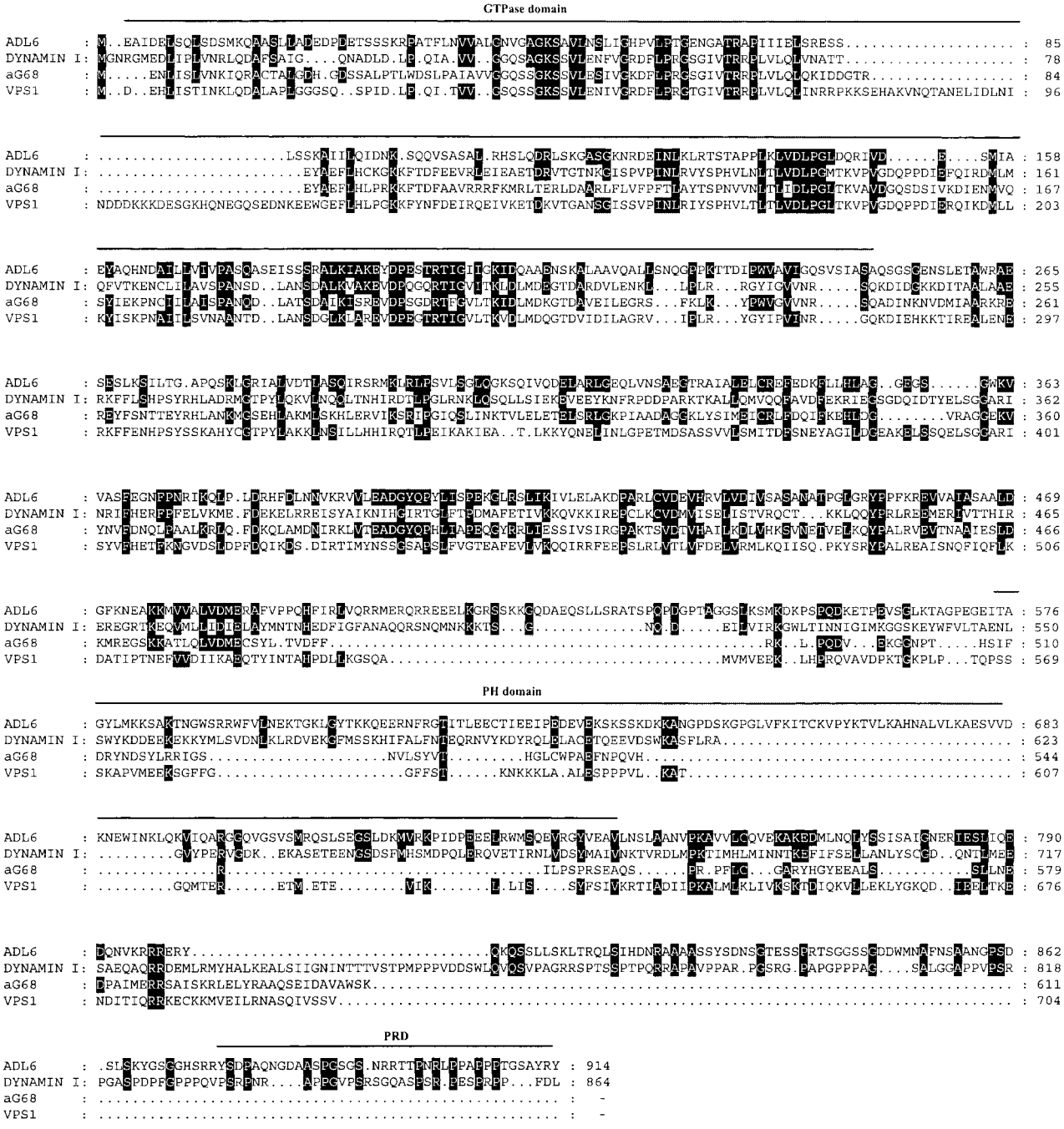

Figure 1. Amino Acid Sequence Alignment of ADL6.

The deduced amino acid sequence of ADL6 was aligned with the sequences of dynamin I, Vps1p, and aG68 using the multiple alignment program of DNASIS (Hitachi, Tokyo, Japan). Gaps were introduced to maximize identity. Identical amino acid residues are indicated by dark shading. The GTPase domain, pleckstrin homology (PH) domain, and Pro-rich domain (PRD) are indicated according to the domains of dynamin I.

(Jiang et al., 2000). Interestingly, precursor-accumulating vesicles have been demonstrated to transport storage proteins to the storage vacuole directly from the ER in pumpkin seeds (Hara-Nishimura et al., 1998). In addition, storage proteins such as vicilin have been shown to be sorted to the storage vacuole at the *cis*-Golgi (Hillmer et al., 2001).

Although recent efforts to unravel the mechanism of intracellular trafficking in plant cells have made significant progress toward understanding the trafficking of cargo molecules to the lytic vacuole (Baba et al., 1997; Frigerio et al., 1998; Zheng et al., 1999; Ahmed et al., 2000; Jiang et al., 2000), the vast majority of molecular players involved in the various steps of intracellular trafficking are still unknown. To understand the mechanism of intracellular trafficking in plant cells, we decided to investigate the proteins involved in vesicle formation. In animal cells, dynamin, a high-molecular-weight GTPase, has been shown to play a critical role in vesicle formation during endocytosis (Obar et al., 1990). The mechanism by which dynamin plays a role in vesicle formation has been well characterized in animal cells (Gout et al., 1993; Herskovits et al., 1993; Damke et al., 1994; Hinshaw and Schmid, 1995; Sweitzer and Hinshaw, 1998; Marks et al., 2001). Vps1p, a homolog of dynamin, also has been shown to be involved in vacuolar targeting of proteins in yeast (Rothman et al., 1990; Bensen et al., 2000). Now, dynamin and related proteins have been isolated from a variety of eukaryotic cells, ranging from yeast to human cells, and have been found to constitute a family of high-molecular-weight-GTP binding proteins (Obar et al., 1990; Rothman et al., 1990; Chen et al., 1991; Dombrowski and Raikhel, 1995; Gu and Verma, 1996; Kang et al., 1998). We previously identified two proteins in Arabidopsis, ADL1 and ADL2, that have a high degree of amino acid sequence homology with dynamin (Kang et al., 1998; Park et al., 1998). However, they are not likely to be involved in vesicle formation during intracellular trafficking because both proteins have been shown to be localized within the chloroplast (Kang et al., 1998; Park et al., 1998). Also, another dynamin homolog, phragmoplastin, found in soybean has been shown to be involved in the formation of the cell division plate (Gu and Verma, 1996, 1997).

Here we report that a new dynamin homolog, Arabidopsis dynamin-like 6 (ADL6), is localized to the Golgi apparatus and is involved in the vacuolar trafficking of cargo proteins from the *trans*-Golgi network (TGN) to the lytic vacuole.

RESULTS

Isolation of the cDNA *ADL6* Encoding Dynamin-Like Protein

A search through the expressed sequence tag (EST) analysis files (University of Minnesota, Plant Molecular Informatics Center) resulted in the identification of 12 EST clones that had significant sequence homology with dynamin. Analysis of these EST clones suggested that there were at least six dynamin-like protein genes in Arabidopsis. A genomic DNA fragment corresponding to the EST clone W43823 was amplified by polymerase chain reaction (PCR) using specific primers corresponding to the 5′ and 3′ ends of the EST clone and used as a hybridization probe to screen an Arabidopsis ZAPII λ cDNA library. Five positive clones were obtained from the screening, and pBluescript SK+ clones were excised from these clones. The cDNA clone was named *ADL6*. The cDNA clone with the largest insert was selected, and the nucleotide sequence was determined using a dye terminator sequencing kit. The nucleotide sequence was deposited in GenBank with the accession number AF180732. The size of the *ADL6* cDNA was 3.21 kb. The first Met codon was located at nucleotide 205 and was followed by an open reading frame of 2.74 kb and an untranslated region of 263 bp.

Sequence Analysis of ADL6

ADL6 has an open reading frame of 2742 bp, which would encode a protein of 914 amino acid residues with a calculated molecular mass of 100 kD. The amino acid sequence of ADL6 reveals the presence of a GTP binding domain at the N terminus, a pleckstrin homology domain in the center, and a Pro-rich SH3 binding domain at the C terminus, indicating that it belongs to the dynamin family of proteins (Obar et al., 1990; Chen et al., 1991). Thus, it appears that ADL6 is more closely related to dynamin I than to other members of the dynamin family with regard to its structural organization. The deduced amino acid sequence of ADL6 also showed a high degree of similarity with other members of the dynamin family; that is, it shared 26% amino acid sequence identity with ADL2 (Kang et al., 1998), 20% with dynamin I (Obar et al., 1990), and 19% with Vps1p (Rothman et al., 1990). The sequence alignments of ADL6 and other dynamin-like proteins are shown in Figure 1.

Subcellular Localization of ADL6

To understand the biological role of ADL6, we next examined its subcellular distribution by protein gel blot analysis. To perform this experiment, we raised a polyclonal antibody against the C-terminal region (amino acid residues 521 to 914) of ADL6 expressed in *Escherichia coli* in rabbits. In whole cell extracts, the antibody specifically recognized one band of ~100 kD, a size that was in good agreement with the calculated molecular mass of the ADL6 gene, whereas the control serum did not detect any protein bands (Figure 2A), suggesting that the antibody was specific to ADL6. However, we often observed an additional weak band right below the major band, and the intensity of the weak band

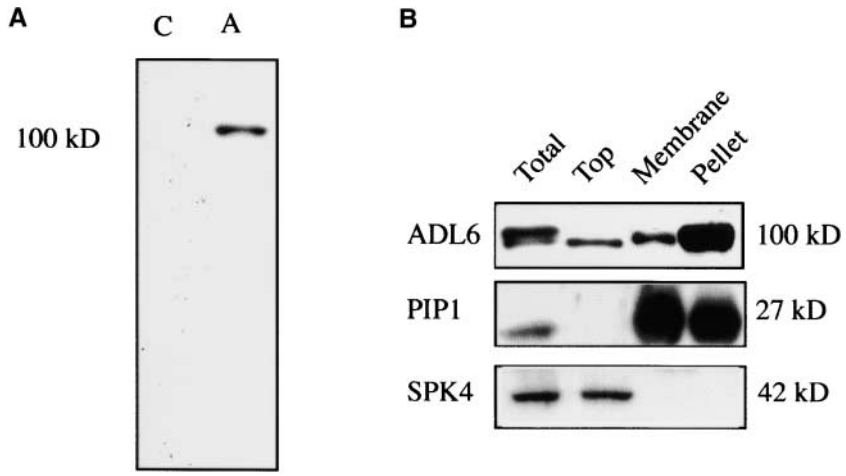

Figure 2. Subcellular Distribution of ADL6.

(A) Specificity of the polyclonal anti-ADL6 antibody. A polyclonal anti-ADL6 antibody was generated in a rabbit using the C-terminal region (amino acids 521 to 914) of ADL6 expressed in *E. coli* as a recombinant protein. Total protein (20 μg) obtained from leaf tissues was separated on an SDS-polyacrylamide gel and transferred onto nylon (polyvinylidene difluoride) membranes. The blots were probed with either the polyclonal anti-ADL6 antibody (A) or a control serum (C).

(B) Subcellular distribution of ADL6. Total protein was fractionated on a Suc step gradient (15, 26, and 35%) by ultracentrifugation. Top, membrane (26/35%), and pellet fractions were collected separately. Twenty micrograms (Total and Top) or 5 μg (Membrane and Pellet) of protein was separated by SDS-PAGE, and protein gel blot analysis was performed with the polyclonal anti-ADL6 antibody. Polyclonal anti-PIP and anti-SPK4 antibodies were used as controls for the fractionation of membrane and soluble fractions, respectively.

(lower band) varied from experiment to experiment. Interestingly, the lower band was present preferentially in the soluble fraction (Figure 2B).

To examine the subcellular distribution of ADL6, whole extracts of Arabidopsis seedlings were fractionated into soluble, membrane, and pellet fractions by Suc step gradient centrifugation, and ADL6 was detected in the various fractions by protein gel blot analysis using the polyclonal anti-ADL6 antibody. Also, to control the quality of fractionation by the Suc step gradient, we used other antibodies, such as polyclonal anti-PIP and anti-SPK4 antibodies (Park et al., 1997), which detect plasma membrane intrinsic protein (PIP) and a soluble soybean protein kinase 4 homolog (SPK-4), respectively. As shown in Figure 2B, ADL6 was present in all fractions. However, the protein species in the upper fraction of the gradient was different from that detected in the membrane and pellet fractions; that is, the lower migrating band predominated in the upper fraction and the upper migrating band predominated in the membrane and pellet fractions.

ADL6 Is Localized to the Golgi Apparatus

To understand the biological role of ADL6, we attempted to localize ADL6 using the anti-ADL6 antibody and a fluorescein isothiocyanate (FITC)–conjugated secondary antibody. Cryosections were prepared from root tips and used for immunolocalization studies. As shown in Figure 3A, the green fluorescent signals of FITC were observed as punctate staining in cortical cells of the root tips (left). However, when the root tips were treated before fixing with brefeldin A (BFA), a Golgi-disrupting agent (Misumi et al., 1986; Fujiwara et al., 1988; Driouich et al., 1993), the punctate staining pattern disappeared and was replaced instead by a diffuse staining pattern (middle), raising the possibility that ADL6 may be associated with the Golgi apparatus. To unequivocally demonstrate its localization, we attempted colocalization with JIM84, a monoclonal antibody that was shown to detect N-glycans with an oligosaccharide sequence of Galβ(1-3)[Fucα(1-4)]GlcNAc at the Golgi apparatus in plant cells (Satiat-Jeunemaitre and Hawes, 1992; Fitchette et al., 1999).

Previously, it was thought that Arabidopsis cells were negative for the JIM84 epitope in the Golgi apparatus. Recently, however, we learned that this epitope can be used as a Golgi marker in Arabidopsis (C. Hawes, personal communication). As shown in Figure 3B, the JIM84 antibody gave a punctate staining pattern in the cortical cells of Arabidopsis root tips (left), indicating that the JIM84 antibody recognizes an epitope in the Golgi apparatus of Arabidopsis, as in other plant cells. In addition, when the tissues were treated with BFA before fixation, the punctate staining pattern detected by JIM84 aggregated into larger spots (middle),

which is another characteristic feature of the glycoprotein detected by JIM84 in the *trans*-Golgi of other plant cells (Satiat-Jeunemaitre and Hawes, 1992; Driouich et al., 1993). This finding further supports the notion that JIM84 can detect the Golgi apparatus in Arabidopsis tissues. However, in contrast to root cells of maize or onion, JIM84 did not label the plasma membrane, indicating that the labeling pattern may be affected by the cell type. In fact, the plasma membranes of BY2 and tomato root tip meristem cells were not labeled with JIM84 (Fitchette et al., 1999). With this information, we

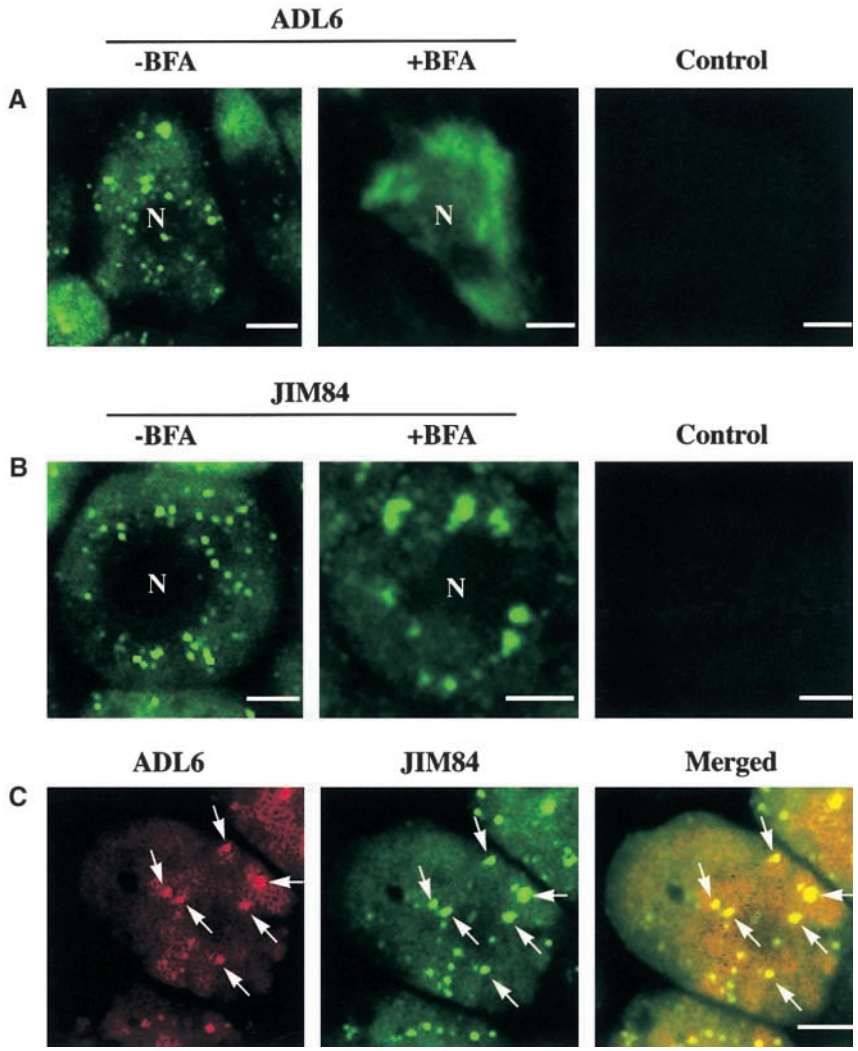

Figure 3. Immunohistochemical Localization of ADL6.

(A) Localization of ADL6. Root tissues of Arabidopsis grown in liquid medium for 1 week were prepared for cryosection. Root tip sections were labeled with the anti-ADL6 antibody as the primary antibody and the FITC-labeled anti-rabbit IgG as the secondary antibody (−BFA). To determine the effect of BFA on the subcellular localization of ADL6, the root tissues were treated with 10 μg/mL BFA for 6 hr before fixation (+BFA). As a control, normal rabbit serum was used as the primary antibody (Control). N, nucleus. Bars = 10 μm.

(B) Localization of JIM84. The root tip sections were labeled with the rat monoclonal antibody JIM84 as the primary antibody followed by FITC-labeled anti-rat IgG as the secondary antibody (−BFA). Also, the root tips were treated with BFA (+BFA) before fixing with 3% glutaraldehyde, and sections were used to determine the effect of BFA on the staining pattern of JIM84. As a control, normal rat serum was used as the primary antibody (Control). N, nucleus. Bars = 10 μm.

(C) Double labeling with anti-ADL6 and JIM84 antibodies. The root tip sections were double labeled as described in Methods. Anti-ADL6 antibody and JIM84 were labeled with tetrathylrhodamine-5-isothiocyanate–labeled anti-rabbit IgG and FITC-labeled anti-rat IgG, respectively. The arrows indicate the overlap of green and red fluorescent signals. Bar = 10 μm.

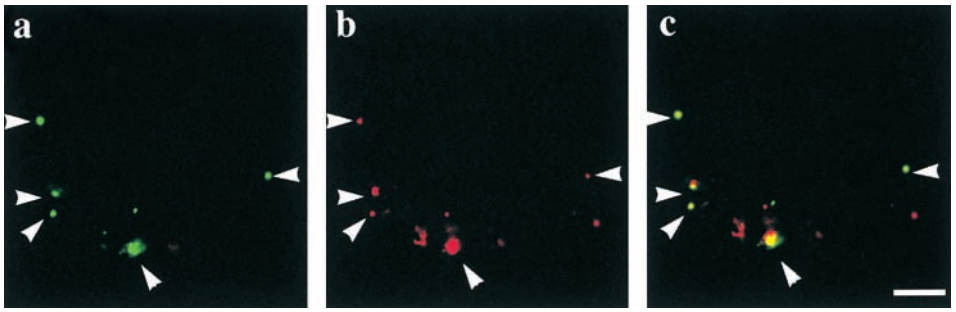

Figure 4. In Vivo Targeting of ADL6.

ADL6:*GFP* was cotransformed into protoplasts with *ST*:*RFP*, and the localization of these proteins was examined at various times after transformation. **(a)**, **(b)**, and **(c)** are images of ADL6:GFP, ST:RFP, and the overlap of ADL6:GFP and ST:RFP, respectively. Arrowheads indicate overlaps of green and red fluorescent signals. Bar = 20 μm.

addressed the question of whether the two punctate staining patterns detected by anti-ADL6 antibody and JIM84 overlapped each other. As shown in Figure 3C, the red (ADL6) and green (JIM84) punctate staining patterns clearly overlapped each other (arrowheads), as indicated by the yellow areas in the merged image, suggesting that ADL6 is localized to the Golgi apparatus.

To obtain independent evidence for the localization of ADL6, we attempted in vivo targeting using an ADL6:green fluorescent protein (GFP) fusion protein. As a marker for the Golgi apparatus, we used rat sialyltransferase fused to red fluorescent protein (ST:RFP) (Wee et al., 1998; Kim et al., 2001). As shown in Figure 4, both ADL6:GFP and ST:RFP gave punctate staining patterns (Figures 4a and 4b), and the majority of green fluorescent signals closely overlapped the red fluorescent signals (Figure 4c). Interestingly, some of the red punctate stains did not overlap the green fluorescent signals of ADL6. However, when we amplified the green signals of ADL6 using image analysis software, we were able to see weak green fluorescent signals at these red punctate stains (data not shown). The difference in the signal intensity of ADL6 at the Golgi apparatus may be attributable to the dynamic nature of ADL6. As in the case of dynamin I, ADL6 also appeared to cycle between soluble dimeric and membrane-associated multimeric forms (J.B. Jin and I. Hwang, unpublished data). Also, when GFP was placed at the N terminus of ADL6, ADL6:GFP gave punctate staining patterns that overlapped ST:RFP (data not shown). Thus, the in vivo targeting experiments further support the notion that ADL6 is localized to the Golgi apparatus.

ADL6 Is Involved in the Trafficking of Cargo Molecules from the TGN to the Central Vacuole

Previously, it was shown that a mutation (K44A) located in the first GTPase binding motif of dynamin I inhibits endocytosis in animal cells by preventing the formation of vesicles from the plasma membrane (Herskovits et al., 1993; Damke et al., 1994). We decided to take a similar mutation-based approach to investigate the biological role of ADL6 by means of an in vivo trafficking assay that uses protoplasts that transiently express reporter proteins destined for various organelles (Kim et al., 2001). An ADL6 mutant, ADL6[K51E], was generated for use as a dominant negative mutant, and the wild-type and mutant proteins were tagged with the T7 epitope at the N terminus (Zheng et al., 1999). Because ADL6 appeared to be localized to the Golgi apparatus, we selected sporamin, a storage protein in the tubers of sweet potato (Hattori et al., 1989), as a cargo protein because it has been shown to be transported to the central vacuole through the Golgi apparatus (Matsuoka et al., 1995; Kim et al., 2001).

We fused GFP to sporamin to facilitate monitoring of the trafficking in the cells. First, we examined the effect of ADL6[K51E] on the trafficking of sporamin:GFP to the central vacuole in protoplasts. As shown in Figure 5A, we usually observed two different patterns of green fluorescent signals when protoplasts were transformed with *sporamin*:*GFP* alone or together with *ADL6*; green fluorescent signals in the central vacuole (Figure 5A, b) indicated that sporamin:GFP had been targeted to its final destination, whereas green fluorescent signals in the ER (Figure 5A, a) indicated that sporamin:GFP had been translated but not yet translocated to its final destination. The localization of untargeted sporamin:GFP to the ER was confirmed by colocalization of sporamin:GFP with chaperone binding protein:red fluorescent protein (BiP:RFP), an ER marker protein (Figure 5A, c) (Kim et al., 2001).

Next, we examined the effect of ADL6[K51E] on the trafficking of sporamin:GFP. When *ADL6[K51E]* was cotransformed into protoplasts, we observed a new punctate staining pattern for sporamin:GFP (Figure 5B, c) in addition to the two patterns of staining seen in the control protoplasts (Figure 5B, a and b). When we carefully examined the whole protoplast population at various times after transformation,

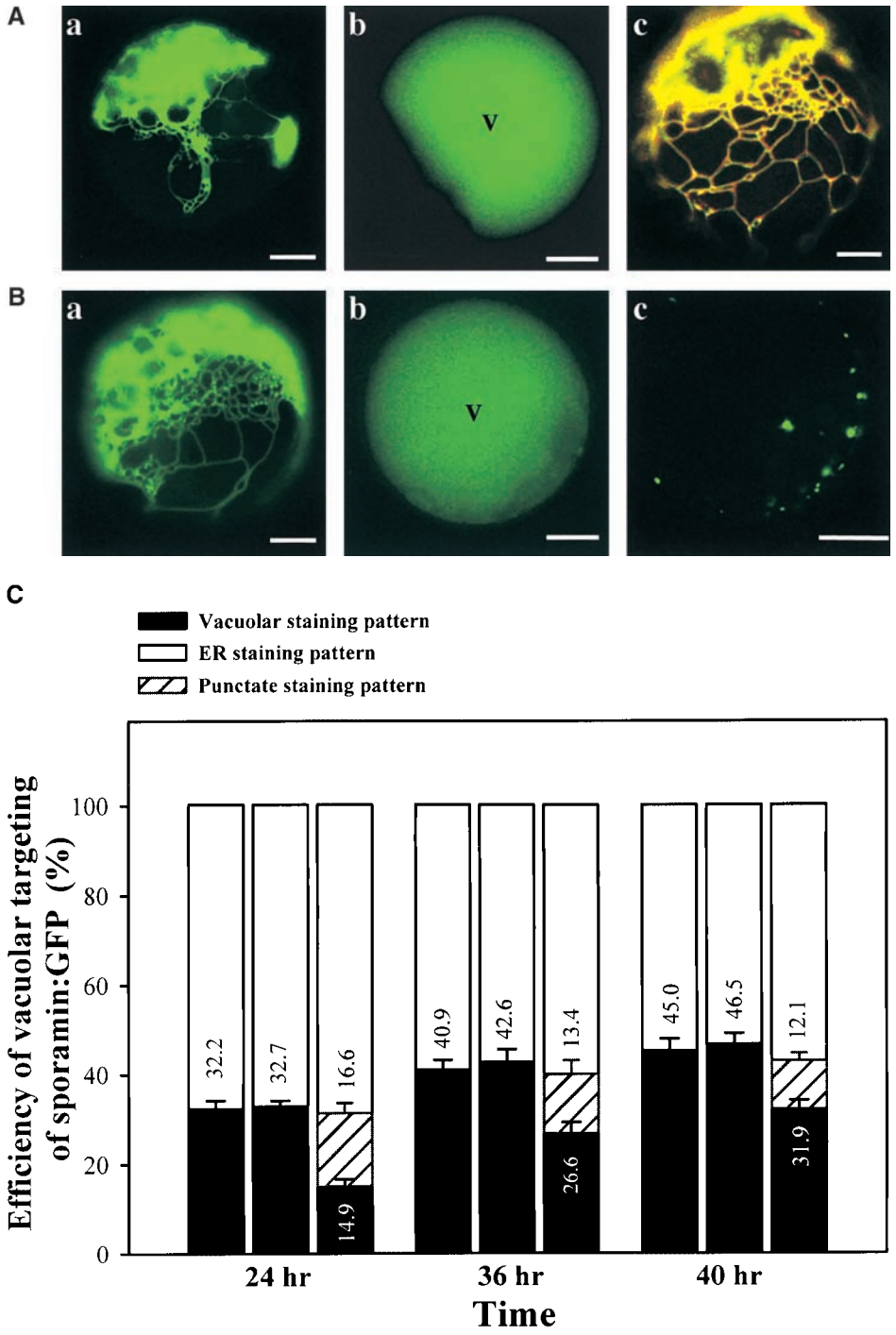

Figure 5. ADL6[K51E] Inhibits Vacuolar Trafficking of Sporamin:GFP.

(A) Trafficking of sporamin:GFP to the central vacuole. Protoplasts were transformed with *sporamin*:*GFP* plus *ADL6* (**[a]** and **[b]**) or *sporamin*:*GFP* plus *ADL6* plus *BiP*:*RFP* **(c)**. **(a)** and **(b)** Two patterns of GFP signals at the ER and central vacuole (V), respectively, 24 hr after transformation. **(c)** Colocalization of sporamin:GFP with BiP:RFP. Yellow color indicates the overlap between green and red fluorescent signals. Bars = 20 μm.
(B) Inhibition of vacuolar trafficking of sporamin:GFP by ADL6[K51E]. Protoplasts were transformed with *sporamin*:*GFP* plus *ADL6[K51E]*. **(a)**, **(b)**, and **(c)** Three types of protoplasts with GFP signals at the ER, the central vacuole, and punctate stains, respectively. V, central vacuole. Bars = 20 μm.
(C) Trafficking efficiency of sporamin:GFP to the central vacuole in the presence of ADL6[K51E]. The whole population of transformed protoplasts was divided into three groups based on GFP signal localization: protoplasts with an ER staining pattern, a punctate staining pattern, or a vacuolar staining pattern. A minimum of 200 transformed protoplasts in each group was counted each time. At least three independent experiments were performed to determine the trafficking efficiency. The first, second, and third columns for each time point indicate protoplasts transformed with *sporamin*:*GFP* alone, *sporamin*:*GFP* plus *ADL6*, and *sporamin*:*GFP* plus *ADL6[K51E]*, respectively. The numbers are means, and the error bars indicate ±SD ($n = 3$).

the percentage of protoplasts with GFP signals in the central vacuole was reduced by as much as 50% compared with protoplasts transformed with *sporamin*:*GFP* alone or with *sporamin*:*GFP* plus *ADL6*, although the targeting efficiency recovered slowly with time (Figure 5C). However, the percentage of transformed protoplasts with GFP signals in the ER was not affected by the presence of ADL6[K51E] (Figure 5C). Thus, these results indicate that the protoplasts with a punctate staining pattern were produced at the expense of the protoplasts with the vacuolar staining pattern.

One possible explanation for this finding would be that ADL6[K51E] inhibits the trafficking of sporamin:GFP to the central vacuole and, as a result, sporamin:GFP is retained in an organelle situated between the ER and the central vacuole. In addition, the punctate staining pattern raised the intriguing possibility that sporamin:GFP may accumulate at the Golgi apparatus in the presence of ADL6[K51E]. To address this possibility, the two constructs, *sporamin*:*GFP* and *ADL6[K51E]*, were introduced into protoplasts together with another construct, *ST*:*RFP* (Kim et al., 2001). As shown in Figure 6A, the red fluorescent signals of ST:RFP at the Golgi apparatus (Figure 6A, b) appeared as punctate stains and clearly overlapped the punctate green fluorescent signals of sporamin:GFP (Figure 6A, c, arrowheads), suggesting that ADL6[K51E] caused the accumulation of sporamin:GFP at the Golgi apparatus, possibly in the region corresponding to the *trans*-Golgi or the TGN. However, to conclude that sporamin:GFP is accumulated at the Golgi apparatus in the

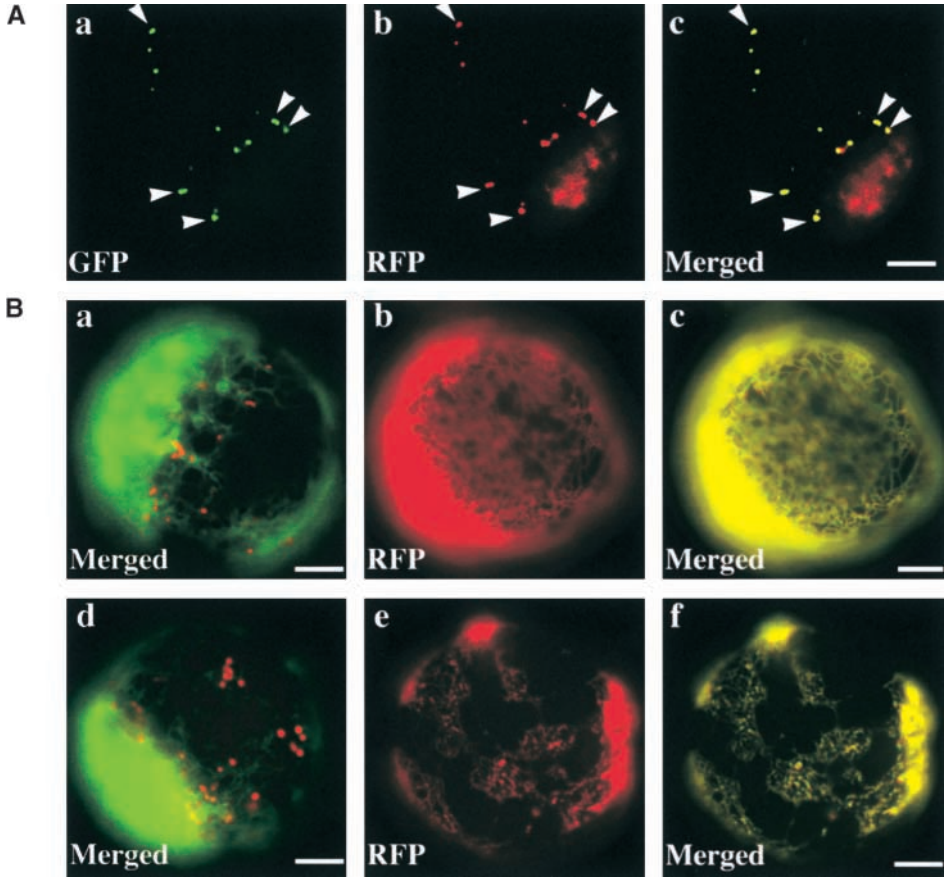

Figure 6. Colocalization of Punctate Staining with ST:RFP at the Golgi Apparatus.

(A) Protoplasts were cotransformed with three constructs, *sporamin*:*GFP*, *ST*:*RFP*, and *ADL6[K51E]*, and the localization of sporamin:GFP **(a)** and ST:RFP **(b)** were examined 24 to 40 hr after transformation. GFP, RFP, and Merged indicate green fluorescent signals, red fluorescent signals, and the overlap of red and green fluorescent signals, respectively. Arrowheads indicate the overlap of red and green fluorescent signals. Bar = 20 μm.

(B) Localization of ST:RFP in the presence of ADL6 and ADL6[K51E]. Protoplasts were transformed with *ST*:*RFP* plus *ADL6* plus *BiP*:*GFP* (**[a]**, **[b]**, and **[c]**) or *ST*:*RFP* plus *ADL6[K51E]* plus *BiP*:*GFP* (**[d]**, **[e]**, and **[f]**), and localization of ST:RFP was examined in the absence (**[a]** and **[d]**) or the presence of BFA (10 μg/mL) (**[b]**, **[c]**, **[e]**, and **[f]**). **(b)** and **(e)** Images of ST:RFP. **(a)**, **(c)**, **(d)**, and **(f)** Merged images between ST:RFP and BiP:GFP. Bars = 20 μm.

presence of ADL6[K51E], it is necessary to show that the expression of ADL6[K51E] does not affect the localization of ST:RFP. To address this question, we compared the staining patterns of ST:RFP in protoplasts expressing ADL6 or ADL6[K51E] and also examined whether ST:RFP can be relocated to the ER in the presence of BFA. Two reporter proteins, ST:RFP and BiP:GFP, were expressed in the presence of ADL6 or ADL6[K51E], and their localization was examined in the absence and presence of BFA. As shown in Figure 6B, in both cases ST:RFP gave punctate staining patterns in the absence of BFA (Figure 6B, a and d), whereas ST:RFP gave diffuse patterns (Figure 6B, b and e) that overlapped BiP:GFP in the presence of BFA (Figure 6B, c and f), indicating that ADL6[K51E] does not affect the localization of ST:RFP at the Golgi apparatus.

To obtain additional evidence for the role of ADL6 in trafficking from the Golgi apparatus to the central vacuole, we selected another cargo protein, endosome binding domain (EBD; the C-terminal region ranging from amino acid residues 1257 to 1411) of human early endosome antigen 1 (Stenmark et al., 1996). The C-terminal EBD that has an Rab5 binding motif and an FYVE zinc finger binding domain has been shown to be responsible for the PI(3)P-dependent localization of early endosome antigen 1 to the endosome. Interestingly, when EBD was expressed as a GFP fusion protein in plant cells, GFP:EBD was transported from the TGN to the central vacuole in a PI(3)P-dependent manner (Kim et al., 2001). As shown in Figure 7A, GFP:EBD was transported to the central vacuole in the presence of ADL6 (Figure 7A, a). When *ADL6[K51E]* was cotransformed with *GFP:EBD*, the targeting efficiency of GFP:EBD was decreased by as much as 50% at 9 hr after transformation compared with that of protoplasts transformed with *GFP:EBD* alone or with *GFP:EBD* plus *ADL6* (Figure 7C). At the same time, we observed an increase in the number of protoplasts with a punctate staining pattern for GFP:EBD (Figure 7A, b). The punctate signals of the green fluorescence of GFP:EBD (Figure 7B, a) clearly overlapped the red fluorescence of ST:RFP (Figure 7B, c, arrowheads), as was the case for sporamin:GFP, indicating that ADL6[K51E] also inhibited trafficking of GFP:EBD to the central vacuole at the TGN. This result was very similar to that found with sporamin:GFP, and, as in that case, the efficiency recovered slowly at later times. This would be expected if the trafficking had not been inhibited completely. Together, these results suggested that ADL6[K51E] had the same inhibitory effect on the two cargo proteins, sporamin:GFP and GFP:EBD, at the TGN.

ADL6[K51E] Does Not Inhibit Trafficking to the Plasma Membrane

To further investigate the specificity of ADL6 involvement in intracellular trafficking, we examined the effect of ADL6[K51E] on the destiny of the integral plasma membrane protein H^+-ATPase:GFP (Kim et al., 2001). As shown in Figure 8, H^+-ATPase:GFP was transported to the plasma membrane in the control protoplasts as expected (Figure 8b). Also, in protoplasts expressing ADL6[K51E] (Figure 8c), H^+-ATPase:GFP was transported to the plasma membrane as efficiently as in the control protoplasts and did not accumulate as a punctate pattern in the cytosol, suggesting that ADL6 is not involved in the trafficking of cargo proteins to the plasma membrane.

To confirm that the difference in the targeting efficiency was attributable to ADL6[K51E], we examined the expression levels of the constructs by performing protein gel blot analysis of protein extracts obtained from the transformed protoplasts. The monoclonal anti-T7 and anti-GFP antibodies were used to detect ADL6 and reporter proteins, respectively. As shown in Figure 9, wild-type and mutant ADL6 were expressed at equal levels. Also, the reporter proteins GFP:EBD (Figure 9A) and sporamin:GFP (Figure 9B) were expressed at nearly equal levels. Thus, this result excluded the possibility that the differential effects of the wild-type and mutant ADL6 proteins on trafficking were caused by a difference in their expression levels.

DISCUSSION

The structural similarity of ADL6 to dynamin I strongly suggests that ADL6 may play a role in vesicle formation at certain membranes. If this is the case, localization of ADL6 could reveal important information about the pathways in which it plays a role. Thus, we first determined the subcellular distribution of ADL6 by subcellular fractionation experiments. When the products of the subcellular fractionation were examined by protein gel blot analysis, the majority of ADL6 was found to be associated with membranes, as in the case of dynamin (Tuma et al., 1993). Interestingly, however, the soluble form of ADL6 migrated slightly ahead of the membrane-bound form. One possible explanation for the difference in the migration rate between the two forms is that ADL6 may be subject to post-translational modification such as phosphorylation. Previously, it was shown that dynamin and dynamin-like proteins are modified by phosphorylation and that they appear as doublets on protein gel blots. The phosphorylated form is found in the soluble fraction and the unmodified form is found in the membrane fraction (Tuma et al., 1993; Park et al., 1997). However, further studies are necessary to understand the difference in the migration rate between the soluble and membrane-bound forms of ADL6.

Next, we established that ADL6 is localized to the Golgi apparatus. This conclusion was based on immunohistochemistry and in vivo targeting. These techniques, however, were not able to reveal the exact location of ADL6 within the Golgi apparatus because of their limited resolution. One possibility is that ADL6 may be localized to the *trans*-Golgi or TGN because N-glycans with an oligosaccharide sequence of Galβ(1-3)[Fucα(1-4)] GlcNAc, the epitope recognized by

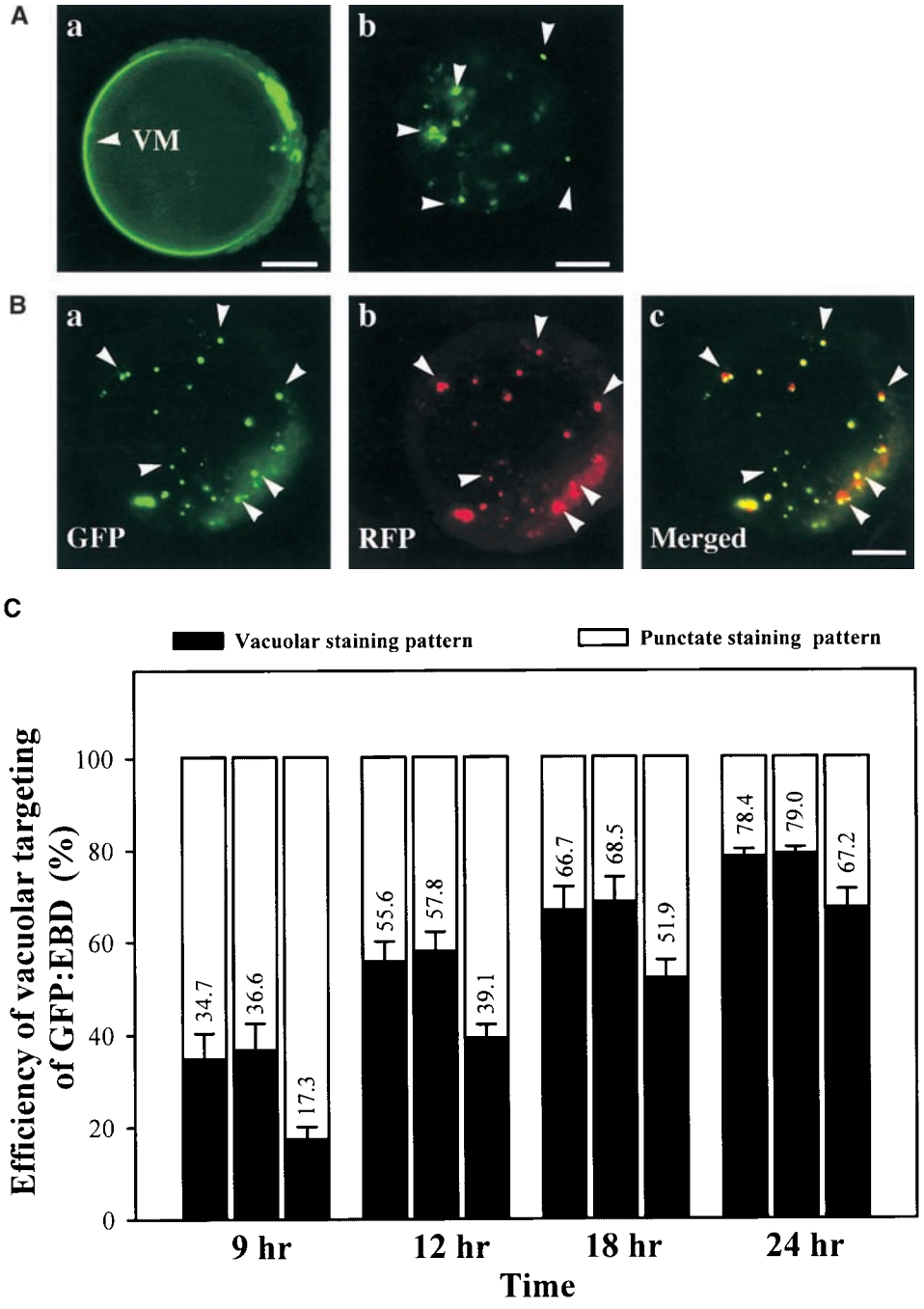

Figure 7. ADL6[K51E] Inhibits Vacuolar Trafficking of GFP:EBD.

(A) Trafficking of GFP:EBD to the central vacuole. *GFP:EBD* was cotransformed into protoplasts with *ADL6* **(a)** or *ADL6[K51E]* **(b)**, and green fluorescent signals of GFP:EBD were examined 24 to 40 hr after transformation. **(a)** A protoplast with GFP:EBD targeted to the central vacuole. **(b)** A protoplast with the punctate staining pattern of GFP:EBD. Arrowheads indicate the punctate stains. VM, vacuole membrane. Bars = 20 μm.

(B) Colocalization of punctate staining with ST:RFP at the Golgi apparatus. Three constructs, *GFP:EBD*, *ST:RFP*, and *ADL6[K51E]*, were cotransformed into protoplasts, and the localization of ST:RFP and GFP:EBD was examined 24 to 40 hr after transformation. GFP, RFP, and Merged indicate green fluorescent signals of GFP:EBD, red fluorescent signals of ST:RFP, and the overlap of green and red fluorescent signals, respectively. Bar = 20 μm.

(C) The trafficking efficiency of GFP:EBD to the central vacuole in the presence of ADL6[K51E]. The whole population of transformed protoplasts was divided into two groups based on the localization of the GFP signals: protoplasts with the vacuolar staining pattern and those with the punctate staining pattern. At least 200 transformed protoplasts in each group were counted each time. At least three independent experiments were performed to determine the trafficking efficiency. The first, second, and third columns for each time point indicate protoplasts transformed with *GFP:EBD* alone, *GFP:EBD* plus *ADL6*, and *GFP:EBD* plus *ADL6[K51E]*, respectively. The numbers are means, and the error bars indicate ±SD ($n = 3$).

the JIM84 antibody, are known to be synthesized at the *trans*-most part of the Golgi apparatus (Fitchette et al., 1999) (see below for further discussion). This location is similar to that of animal dynamin II, which has been shown to be localized to the TGN and to play roles in post-Golgi trafficking (Henley and McNiven, 1996; Maier et al., 1996; Cao et al., 1998; Jones et al., 1998). Also, Vps1p, which plays a role in vacuolar trafficking, has been shown to be localized to the Golgi apparatus in yeast (Wilsbach and Payne, 1993). However, this is in contrast to dynamin I, which is localized to the plasma membrane in animal cells (Herskovits et al., 1993; Robinson et al., 1993; Sweitzer and Hinshaw, 1998).

Among the members of the dynamin family, the molecular mechanism by which dynamin I plays a role during endocytosis has been best characterized. Dynamin I is recruited and assembled into rings at the necks of clathrin-coated buds at the plasma membrane, and a conformational change of the dynamin rings results in the severance of the necks to release the buds as vesicles during endocytosis (Herskovits et al., 1993; Robinson et al., 1993; Sweitzer and Hinshaw, 1998). Given its homology with dynamin I, ADL6 may play a role at the Golgi apparatus, and possibly at the TGN, similar to that which dynamin I plays at the plasma membrane. In fact, some vacuolar cargo proteins have been shown to leave the TGN in clathrin-coated vesicles in plant cells (Hohl et al., 1996; Robinson et al., 1998).

To address this possibility, we examined the effect of a dominant negative mutant of ADL6 on the vacuolar trafficking of cargo proteins in protoplasts, a strategy that had already been successful in revealing the role of human dynamin I (Herskovits et al., 1993; Damke et al., 1994). The dominant negative mutant of dynamin I causes inhibition of endocytosis in animal cells. Similarly, in the presence of ADL6[K51E], we observed significant inhibition of the vacuolar trafficking of two reporter proteins: sporamin:GFP, a reporter protein transported to the lytic vacuole through the ER and the Golgi apparatus (Matsuoka et al., 1995; Kim et al., 2001), and GFP:EBD, a reporter protein that is transported from the TGN to the lytic vacuole (Kim et al., 2001). At the same time, we observed a concomitant increase in the punctate distribution of these reporters, which was found to represent the Golgi apparatus.

The accumulation of cargo proteins at the Golgi apparatus was in good agreement with the proposed role of ADL6. In animal cells expressing the dominant negative mutant, transferrin accumulated in a punctate fashion at the plasma membrane, as indicated by the fact that vesicles were not released from it (Herskovits et al., 1993; Damke et al., 1994). Similarly, vesicles may not be released from the Golgi apparatus in the presence of the dominant negative mutant of ADL6. The inhibition of both reporter proteins at the Golgi apparatus strongly suggests that ADL6 plays a role at the TGN and that the cargo proteins may have accumulated at the TGN in the presence of the mutant protein. This conclusion is based on the fact that, unlike sporamin:GFP, GFP:EBD is expressed in the cytosol, is recruited to the TGN in a PI(3)P-dependent manner, and then is transported to the central vacuole but is not transported through the Golgi apparatus (Kim et al., 2001).

In plant cells, there are other routes that vesicles derived from the Golgi apparatus can take to transport cargo proteins. One example is the trafficking pathway from the Golgi apparatus to the plasma membrane (Hawes et al., 1999). In contrast to vacuolar trafficking, ADL6[K51E] did not affect the trafficking of H^+-ATPase:GFP to the plasma membrane, suggesting that ADL6 is not involved in trafficking from the Golgi apparatus to the plasma membrane.

Recently, protein components involved in trafficking from the TGN to the lytic vacuole have been identified. These include BP80, AtELP, AtVTI1a, AtPEP12p, AtVAMP3p, and AtVPS45 (Paris et al., 1997; Bassham and Raikhel, 1999; Zheng et al., 1999; Ahmed et al., 2000; Bassham et al., 2000). Among these proteins, AtELP, a putative cargo receptor, has been shown to be localized to the TGN and is thought to be involved in the vacuolar trafficking of cargo proteins from the TGN (Ahmed et al., 2000). Thus, one possibility is

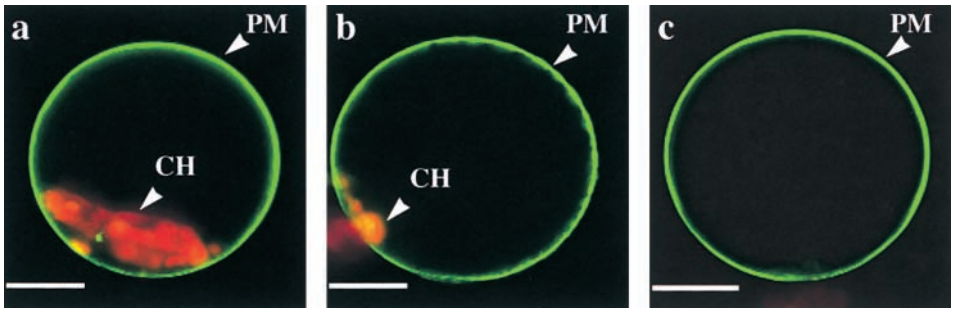

Figure 8. ADL6[K51E] Does Not Inhibit the Trafficking of H^+-ATPase:GFP to the Plasma Membrane.

Protoplasts were transformed with *H^+-ATPase*:*GFP* alone **(a)**, *H^+-ATPase*:*GFP* plus *ADL6* **(b)**, or *H^+-ATPase*:*GFP* plus *ADL6[K51E]* **(c)**, and green fluorescent signals of H^+-ATPase:GFP were examined at various times. PM and CH indicate the plasma membrane and chloroplasts, respectively. Bars = 25 μm.

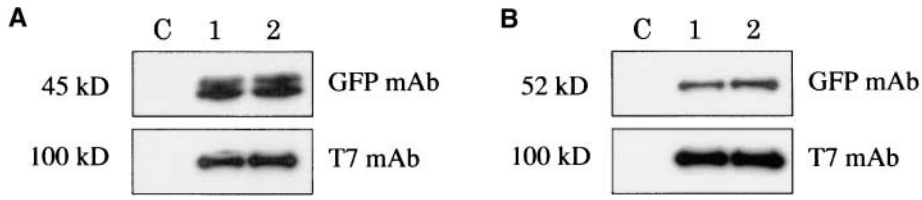

Figure 9. Expression Levels of the Constructs in Protoplasts.

Total protein extracts were prepared from protoplasts transformed with various constructs and separated on an SDS-polyacrylamide gel for protein gel blot analysis. The blots were probed with monoclonal anti-T7 (T7 mAb) and anti-GFP (GFP mAb) antibodies to detect the T7 epitope-tagged ADLs and GFP-tagged reporter proteins, respectively. The expected sizes of proteins are indicated.

(A) C, 1, and 2 indicate untransformed protoplasts, protoplasts transformed with *T7*:*ADL6* plus *GFP*:*EBD*, and protoplasts transformed with *T7*:*ADL6[K51E]* plus *GFP*:*EBD*, respectively.

(B) C, 1, and 2 indicate untransformed protoplasts, protoplasts transformed with *T7*:*ADL6* plus *sporamin*:*GFP*, and protoplasts transformed with *T7*:*ADL6[K51E]* plus *sporamin*:*GFP*, respectively.

that ADL6 may play a role in the formation of vesicles that are induced by AtELP at the TGN. Further studies will be necessary to prove the exact relationship between AtELP and ADL6 during vacuolar trafficking in plant cells.

In this study, we used sporamin:GFP and GFP:EBD as cargo proteins for the in vivo trafficking assay in Arabidopsis protoplasts. Sporamin, a storage protein found in the tubers of sweet potato, has been shown to be transported to the lytic vacuole in heterologous systems such as tobacco (Matsuoka et al., 1995; Kim et al., 2001). Also, GFP:EBD has been shown to be transported to the lytic vacuole from the TGN in a PI(3)P-dependent manner in Arabidopsis (Kim et al., 2001). When we expressed the sporamin:GFP in Arabidopsis protoplasts, the targeting efficiency to the lytic vacuole was ~50% at 40 hr after transformation. However, the efficiency was increased to 70 to 80% at 72 hr (data not shown). In contrast, the targeting efficiency of GFP:EBD and H^+-ATPase:GFP was nearly 80 and 95%, respectively, at 24 hr after transformation (data not shown for H^+-ATPase:GFP), indicating that the targeting efficiency is dependent on the reporter proteins. One possible explanation for the slower trafficking of sporamin is that protoplasts prepared from Arabidopsis leaf cells (a heterologous system for the expression of sporamin) may have a limited supply of the necessary machinery or of one of its components. In fact, the targeting efficiency was increased to nearly 70% at 12 hr after transformation when Seh1h, a polypeptide that interacts with ADL6, was expressed in the protoplasts (S.H. Lee and I. Hwang, unpublished data).

METHODS

Growth of Plants

Arabidopsis thaliana (ecotype Columbia) was grown either on Murashige and Skoog (1962) plates at 20°C in a culture room or in a greenhouse under conditions of 70% RH and a 16-hr-light/8-hr-dark cycle.

Screening of a cDNA Encoding Dynamin-Like Protein

A probe for screening of cDNAs encoding dynamin-like proteins in Arabidopsis was prepared by polymerase chain reaction (PCR) amplification using primers designed from the nucleotide sequence information deposited in the expressed sequence tag (EST) database (GenBank accession number W43823). The primers were as follows: ADL6-5, 5′-TGCTAGTCGCGATGGAG-3′; ADL6-3, 5′-CTCGTGTAGCACCATTC-3′. PCR amplification and library screening were performed as described previously (Kang et al., 1998).

Preparation of Membrane Fractions

Protein extracts were prepared and fractionated by a Suc step gradient according to Park et al. (1997). The presence of Arabidopsis dynamin-like 6 (ADL6) in fractions collected from the gradient was detected using the polyclonal anti-ADL6 antibody.

Preparation of Antibody and Protein Gel Blot Analysis

For protein gel blot analysis, a polyclonal antibody was raised against a truncated form of ADL6. The C-terminal region of ADL6 (393 amino acid residues) was expressed in *Escherichia coli* as a recombinant protein using the expression vector pRSET-B (Invitrogen, Carlsbad, CA). The recombinant protein was expressed and purified according to the manufacturer's protocol. The purified protein was injected into a rabbit to raise antibody according to a published protocol (Harlow and Lane, 1988). The polyclonal antibody was purified and used for protein gel blot analysis according to Park et al. (1997). The blots were developed using an enhanced chemiluminescence detection system for protein gel blots (Amersham).

Immunocytohistochemistry

Cryosections were prepared from root tissues of Arabidopsis grown in liquid Murashige and Skoog (1962) medium as described previously (Wick, 1993) and then immunolabeled as described previously (Gindullis and Meier, 1999). The root tissues also were treated with brefeldin A (BFA) (10 μg/mL) before fixation. The purified anti-ADL6

antibody and fluorescein isothiocyanate (FITC)-labeled anti-rabbit IgG were used as primary and secondary antibodies, respectively. For double labeling, a mixture of a monoclonal antibody, JIM84 (Satiat-Jeunemaitre and Hawes, 1992), and an anti-ADL6 antibody was used as the primary antibody, and then the sections were stained sequentially with FITC-labeled anti-rat IgG and tetrathylrhodamine-5-isothiocyanate–labeled anti-rabbit IgG. Images were observed using a Zeiss (Jena, Germany) Axioplan fluorescence microscope.

Generation of Constructs

ADL6[K51E] was generated by PCR using primers 5′-CTGCAGACTCTCCAGCTCCCACATTTCC-3′ and 5′-TGCTAGTCGCGATGGAG-3′. The T7 epitope tag also was added to the N terminus of ADL6 by PCR using primers 5′-ACTGGTGGACAGCAAATGGGTCGCGGATCCATGGAGGCGATCGATGAG-3′ and 5′-AAAGAGTAAAGAAGAACAATGGCTAGCATGACTGGTGGACAGCAAATG-3′. The PCR products were confirmed by nucleotide sequencing. The ADL6 constructs were placed under the control of the 35S cauliflower mosaic virus promoter in a pUC vector. The ADL6:green fluorescent protein (GFP) fusion construct was generated by placing the ADL6 coding region in frame to the C terminus of the GFP coding region without the termination codon.

In Vivo Targeting of Green and Red Fluorescent Protein Fusion Constructs

Plasmids were purified using Qiagen (Valencia, CA) columns according to the manufacturer's protocol. The fusion constructs were introduced into Arabidopsis protoplasts prepared from whole seedlings by polyethylene glycol–mediated transformation (Kang et al., 1998). Briefly, leaf tissues (5 g) of 3- to 4-week-old Arabidopsis plants grown on soil in a greenhouse were cut into small squares (5 to 10 mm^2) with a new razor blade and incubated with 50 mL of enzyme solution (0.25% Macerozyme (Yakult Honsha Co., Ltd., Tokyo, Japan) R-10, 1.0% Cellulase (Yakult Honsha Co., Ltd.) R-10, 400 mM mannitol, 8 mM $CaCl_2$, and 5 mM Mes-KOH, pH 5.6) at 22°C for 5 hr with gentle agitation (50 to 75 rpm). After incubation, the protoplast suspension was filtered through 100-μm mesh and protoplasts were collected by centrifugation at 46*g* for 5 min. The pelleted protoplasts were resuspended in 5 to 10 mL of W5 solution (154 mM NaCl, 125 mM $CaCl_2$, 5 mM KCl, 5 mM glucose, and 1.5 mM Mes-KOH, pH 5.6), overlaid on top of 20 mL of 21% Suc, and centrifuged for 10 min at 78*g*. The intact protoplasts at the interface were transferred to a new Falcon tube containing 20 mL of W5 solution. The protoplasts were pelleted again by centrifugation at 55*g* for 5 min and resuspended in 20 mL of W5 solution. The protoplasts were incubated on ice for 30 min.

To transform DNA into protoplasts, protoplasts were pelleted again at 46*g* for 5 min and resuspended in MaMg solution (400 mM mannitol, 15 mM $MgCl_2$, and 5 mM Mes-KOH, pH 5.6) at a density of 5×10^6 protoplasts/mL. Plasmid DNA (20 to 50 μg total at a concentration of 2 mg/mL) was added to 300 μL of protoplast suspension followed by 325 μL of PEG solution [400 mM mannitol, 100 mM $Ca(NO_3)_2$, and 40% polyethylene glycol 4000]. The mixture was mixed gently and incubated for 30 min at room temperature. After incubation, the mixture was diluted with 10 mL of W5 solution. Protoplasts were recovered by centrifugation at 50*g* for 5 min, resuspended in 3 mL of W5 solution, and incubated at 22°C in the dark. Expression of protein was monitored at various times after transformation, and images were captured with a cooled charge-coupled device camera using a Zeiss Axioplan fluorescence microscope. The filter sets used were XF116 (exciter, 474AF20; dichroic, 500DRLP; emitter, 510AF23), XF33/E (exciter, 535DF35; dichroic, 570DRLP; emitter, 605DF50), and XF137 (exciter, 540AF30; dichroic, 570DRLP; emitter, 585ALP) (Omega, Inc., Brattleboro, VT) for green fluorescent protein, red fluorescent protein, and autofluorescence of chlorophyll, respectively. Data were then processed using Adobe (Mountain View, CA) Photoshop software, and the images were rendered in pseudocolor.

ACKNOWLEDGMENTS

We thank C. Hawes (Oxford Brookes University, Oxford, UK) for the monoclonal antibody JIM84 and for the personal communication regarding the localization of the epitope detected by JIM84. Also, we thank Dr. Soon-Ok Eun (Pohang University of Science and Technology, Pohang, Korea) for technical help in immunohistochemical labeling. This work was supported by a grant from the National Creative Research Initiatives of the Ministry of Science and Technology in Korea.

Received December 15, 2000; accepted April 29, 2001.

REFERENCES

Ahmed, S.U., Rojo, E., Kovaleva, V., Venkataraman, S., Dombrowski, J.E., Matsuoka, K., and Raikhel, N.V. (2000). The plant vacuolar sorting receptor AtELP is involved in transport of NH(2)-terminal propeptide-containing vacuolar proteins in *Arabidopsis thaliana*. J. Cell Biol. **149,** 1335–1344.

Baba, M., Osumi, M., Scott, S.V., Klionsky, D.J., and Ohsumi, Y. (1997). Two distinct pathways for targeting proteins from the cytoplasm to the vacuole/lysosome. J. Cell Biol. **139,** 1687–1695.

Bassham, D.C., and Raikhel, N.V. (1999). The pre-vacuolar t-SNARE AtPEP12p forms a 20S complex that dissociates in the presence of ATP. Plant J. **19,** 599–603.

Bassham, D.C., and Raikhel, N.V. (2000). Unique features of the plant vacuolar sorting machinery. Curr. Opin. Cell Biol. **12,** 491–495.

Bassham, D.C., Gal, S., da Silva Conceicao, A., and Raikhel, N.V. (1995). An Arabidopsis syntaxin homologue isolated by functional complementation of a yeast pep12 mutant. Proc. Natl. Acad. Sci. USA **92,** 7262–7266.

Bassham, D.C., Sanderfoot, A.A., Kovaleva, V., Zheng, H., and Raikhel, N.V. (2000). AtVPS45 complex formation at the *trans*-Golgi network. Mol. Biol. Cell. **11,** 2251–2265.

Bensen, E.S., Costaguta, G., and Payne, G.S. (2000). Synthetic genetic interactions with temperature-sensitive clathrin in *Saccharomyces cerevisiae*: Roles for synaptojanin-like Inp53p and dynamin-related Vps1p in clathrin-dependent protein sorting at the *trans*-Golgi network. Genetics **154,** 83–97.

Blackbourn, H.D., and Jackson, A.P. (1996). Plant clathrin heavy chain: Sequence analysis and restricted localisation in growing pollen tubes. J. Cell Sci. **109,** 777–786.

Cao, H., Garcia, F., and McNiven, M.A. (1998). Differential distribution of dynamin isoforms in mammalian cells. Mol. Biol. Cell **9,** 2595–2609.

Chen, M.S., Obar, R.A., Schroeder, C.C., Austin, T.W., Poodry, C.A., Wadsworth, S.C., and Vallee, R.B. (1991). Multiple forms of dynamin are encoded by *shibire*, a *Drosophila* gene involved in endocytosis. Nature **351,** 583–586.

Damke, H., Baba, T., Warnock, D.E., and Schmid, S.L. (1994). Induction of mutant dynamin specifically blocks endocytic coated vesicle formation. J. Cell Biol. **127,** 915–934.

Dombrowski, J.E., and Raikhel, N.V. (1995). Isolation of a cDNA encoding a novel GTP-binding protein of *Arabidopsis thaliana*. Plant Mol. Biol. **28,** 1121–1126.

Driouich, A., Zhang, G.F., and Staehelin, L.A. (1993). Effect of brefeldin A on the structure of the Golgi apparatus and on the synthesis and secretion of proteins and polysaccharides in sycamore maple (*Acer pseudoplatanus*) suspension-cultured cells. Plant Physiol. **101,** 1363–1373.

Fitchette, A.C., Cabanes-Macheteau, M., Marvin, L., Martin, B., Satiat-Jeunemaitre, B., Gomord, V., Crooks, K., Lerouge, P., Faye, L., and Hawes, C. (1999). Biosynthesis and immunolocalization of Lewis a-containing N-glycans in the plant cell. Plant Physiol. **121,** 333–344.

Frigerio, L., de Virgilio, M., Prada, A., Faoro, F., and Vitale, A. (1998). Sorting of phaseolin to the vacuole is saturable and requires a short C-terminal peptide. Plant Cell **10,** 1031–1042.

Fujiwara, T., Oda, K., Yokota, S., Takatsuki, A., and Ikehara, Y. (1988). Brefeldin A causes disassembly of the Golgi complex and accumulation of secretory proteins in the endoplasmic reticulum. J. Biol. Chem. **263,** 18545–18552.

Gindullis, F., and Meier, I. (1999). Matrix attachment region binding protein MFP1 is localized in discrete domains at the nuclear envelope. Plant Cell **11,** 1117–1128.

Gout, I., Dhand, R., Hiles, I.D., Fry, M.J., Panayotou, G., Das, P., Truong, O., Totty, N.F., Husan, J., Booker, G.W., Campbell, I.D., and Waterfield, M.D. (1993). The GTPase dynamin binds to and is activated by a subset of SH3 domains. Cell **75,** 25–36.

Gu, X., and Verma, D.P.S. (1996). Phragmoplastin, a dynamin-like protein associated with cell plate formation in plants. EMBO J. **15,** 695–704.

Gu, X., and Verma, D.P. (1997). Dynamics of phragmoplastin in living cells during cell plate formation and uncoupling of cell elongation from the plane of cell division. Plant Cell **9,** 157–169.

Hara-Nishimura, I., Shimada, T., Hatano, K., Takeuchi, Y., and Nishimura, M. (1998). Transport of storage proteins to protein storage vacuoles is mediated by large precursor-accumulating vesicles. Plant Cell **10,** 825–836.

Harlow, E., and Lane, D. (1988). Antibodies: A Laboratory Manual. (Cold Spring Harbor, NY: Cold Spring Harbor Laboratory Press).

Hattori, T., Yoshida, N., and Nakamura, K. (1989). Structural relationship among the members of a multigene family coding for the sweet potato tuberous root storage protein. Plant Mol. Biol. **13,** 563–572.

Hawes, C.R., Brandizzi, F., and Andreeva, A.V. (1999). Endomembranes and vesicle trafficking. Curr. Opin. Plant Biol. **2,** 454–461.

Henley, J.R., and McNiven, M.A. (1996). Association of a dynamin-like protein with the Golgi apparatus in mammalian cells. J. Cell Biol. **133,** 761–775.

Herskovits, J.S., Burgess, C.C., Obar, R.A., and Vallee, R.B. (1993). Effects of mutant rat dynamin on endocytosis. J. Cell Biol. **122,** 565–578.

Hillmer, S., Movafeghi, A., Robinson, D.G., and Hinz, G. (2001). Vacuolar storage proteins are sorted in the *cis*-cisternae of the pea cotyledon Golgi apparatus. J. Cell Biol. **152,** 41–50.

Hinshaw, J.E., and Schmid, S.L. (1995). Dynamin self-assembles into rings suggesting a mechanism for coated vesicle budding. Nature **374,** 190–192.

Hohl, I., Robinson, D.G., Chrispeels, M.J., and Hinz, G. (1996). Transport of storage proteins to the vacuole is mediated by vesicles without a clathrin coat. J. Cell Sci. **109,** 2539–2550.

Jahn, R., and Südhof, T.C. (1999). Membrane fusion and exocytosis. Annu. Rev. Biochem. **68,** 863–911.

Jiang, L., Phillips, T.E., Rogers, S.W., and Rogers, J.C. (2000). Biogenesis of the protein storage vacuole crystalloid. J. Cell Biol. **150,** 755–770.

Jones, S.M., and Howell, K.E. (1997). Phosphatidylinositol 3-kinase is required for the formation of constitutive transport vesicles from the TGN. J. Cell Biol. **139,** 339–349.

Jones, S.M., Howell, K.E., Henley, J.R., Cao, H. and McNiven, M.A. (1998). Role of dynamin in the formation of transport vesicles from the *trans*-Golgi network. Science **279,** 573–577.

Kang, S.G., Jin, J.B., Piao, H.L., Pih, K.T., Jang, H.J., Lim, J.H., and Hwang, I. (1998). Molecular cloning of an *Arabidopsis* cDNA encoding a dynamin-like protein that is localized to plastids. Plant Mol. Biol. **38,** 437–447.

Kim, D.H., Eu, Y.-J., Yoo, C.M., Kim, Y.W., Pih, K.T., Jin, J.B., Kim, S.J., Stenmark, H., and Hwang, I. (2001). Trafficking of phosphatidylinositol 3-phosphate from the *trans*-Golgi network to the lumen of the central vacuole in plant cells. Plant Cell **13,** 287–301.

Lebas, M., and Axelos, M. (1994). A cDNA encoding a new GTP-binding protein of the ADP-ribosylation factor family from *Arabidopsis*. Plant Physiol. **106,** 809–810.

Maier, O., Knoblich, M., and Westermann, P. (1996). Dynamin II binds to the *trans*-Golgi network. Biochem. Biophys. Res. Commun. **223,** 229–233.

Marks, B., Stowell, M.H., Vallis, Y., Mills, I.G., Gibson, A., Hopkins, C.R., and McMahon, H.T. (2001). GTPase activity of dynamin and resulting conformation change are essential for endocytosis. Nature **410,** 231–235.

Matsuoka, K., Watanabe, N., and Nakamura, K. (1995). *O*-Glycosylation of a precursor to a sweet potato vacuolar protein, sporamin, expressed in tobacco cells. Plant J. **8,** 877–889.

Misumi, Y., Misumi, Y., Miki, K., Takatsuki, A., Tamura, G., and Ikehara, Y. (1986). Novel blockade by brefeldin A of intracellular transport of secretory proteins in cultured rat hepatocytes. J. Biol. Chem. **261,** 11398–11403.

Movafeghi, A., Happel, N., Pimpl, P., Tai, G.H., and Robinson, D.G. (1999). Arabidopsis Sec21p and Sec23p homologs: Probable coat proteins of plant COP-coated vesicles. Plant Physiol. **119,** 1437–1446.

Murashige, T., and Skoog, F. (1962). A revised medium for rapid growth and bioassays with tobacco tissue culture. Physiol. Plant. **15,** 473–497.

Neuhaus, J.M., and Rogers, J.C. (1998). Sorting of proteins to vacuoles in plant cells. Plant Mol. Biol. **38,** 127–144.

Obar, R.A., Collins, C.A., Hammarback, J.A., Shpetner, H.S., and Vallee, R.B. (1990). Molecular cloning of the microtubule-associated mechanochemical enzyme dynamin reveals homology with a new family of GTP-binding proteins. Nature **347,** 256–261.

Paris, N., Rogers, S.W., Jiang, L., Kirsch, T., Beevers, L., Phillips, T.E., and Rogers, J.C. (1997). Molecular cloning and further characterization of a probable plant vacuolar sorting receptor. Plant Physiol. **115,** 29–39.

Park, J.M., Kang, S.G., Pih, K.T., Jang, H.J., Piao, H.L., Yoon, H.W., Cho, M.J., and Hwang, I. (1997). A dynamin-like protein, ADL1, is present in membranes as a high-molecular-mass complex in *Arabidopsis thaliana*. Plant Physiol. **115,** 763–771.

Park, J.M., Cho, J.H., Kang, S.G., Jang, H.J., Pih, K.T., Piao, H.L., Cho, M.J., and Hwang, I. (1998). A dynamin-like protein in *Arabidopsis thaliana* is involved in biogenesis of thylakoid membranes. EMBO J. **17,** 859–867.

Pimpl, P., Movafeghi, A., Coughlan, S., Denecke, J., Hillmer, S., and Robinson, D.G. (2000). In situ localization and in vitro induction of plant COPI-coated vesicles. Plant Cell **12,** 2219–2236.

Robinson, D.G., Hinz, G., and Holstein, S.E. (1998). The molecular characterization of transport vesicles. Plant Mol. Biol. **38,** 49–76.

Robinson, P.J., Sontag, J.-M., Liu, J.-P., Fykse, E.S., Slaughter, C., McMahon, H., and Sudhof, T.C. (1993). Dynamin GTPase regulated by protein kinase C phosphorylation in nerve terminals. Nature **365,** 163–166.

Rothman, J.E. (1994). Mechanisms of intracellular protein import. Nature **372,** 55–63.

Rothman, J.H., Raymond, C.K., Gilbert, T., O'Hara, P.J., and Stevens, T.H. (1990). A putative GTP binding protein homologous to interferon-inducible Mx proteins performs an essential function in yeast protein sorting. Cell **61,** 1063–1074.

Sanderfoot, A.A., Assaad, F.F., and Raikhel, N.V. (2000). The Arabidopsis genome: An abundance of soluble *N*-ethylmaleimide-sensitive factor adaptor protein receptors. Plant Physiol. **124,** 1558–1569.

Satiat-Jeunemaitre, B., and Hawes, C. (1992). Redistribution of a Golgi glycoprotein in plant cells treated with brefeldin A. J. Cell Sci. **103,** 1153–1166.

Schu, P.V., Takegawa, K., Fry, M.J., Stack, J.H., Waterfield, M.D., and Emr, S.D. (1993). Phosphatidylinositol 3-kinase encoded by yeast VPS34 gene essential for protein sorting. Science **260,** 88–91.

Sever, S., Muhlberg, A.B., and Schmid, S.L. (1999). Impairment of dynamin's GAP domain stimulates receptor-mediated endocytosis. Nature **398,** 481–486.

Stenmark, H., Aasland, R., Toh, B.H., and D'Arrigo, A. (1996). Endosomal localization of the autoantigen EEA1 is mediated by a zinc-binding FYVE finger. J. Biol. Chem. **271,** 24048–24054.

Sweitzer, S.M., and Hinshaw, J.E. (1998). Dynamin undergoes a GTP-dependent conformational change causing vesiculation. Cell **93,** 1021–1029.

Takeuchi, M., Tada, M., Saito, C., Yashiroda, H., and Nakano, A. (1998). Isolation of a tobacco cDNA encoding Sar1 GTPase and analysis of its dominant mutations in vesicular traffic using a yeast complementation system. Plant Cell Physiol. **39,** 590–599.

Takeuchi, M., Ueda, T., Sato, K., Abe, H., Nagata, T., and Nakano, A. (2000). A dominant negative mutant of sar1 GTPase inhibits protein transport from the endoplasmic reticulum to the Golgi apparatus in tobacco and Arabidopsis cultured cells. Plant J. **23,** 517–525.

Toyooka, K., Okamoto, T., and Minamikawa, T. (2000). Mass transport of proform of a KDEL-tailed cysteine proteinase (SH-EP) to protein storage vacuoles by endoplasmic reticulum-derived vesicle is involved in protein mobilization in germinating seeds. J. Cell Biol. **148,** 453–464.

Tuma, P.L., Stachniak, M.C., and Collins, C.A. (1993). Activation of dynamin GTPase by acidic phospholipids and endogenous rat brain vesicles. J. Biol. Chem. **268,** 17240–17246.

Wee, E.G., Sherrier, D.J., Prime, T.A., and Dupree, P. (1998). Targeting of active sialyltransferase to the plant Golgi apparatus. Plant Cell **10,** 1759–1768.

Wick, S.M. (1993). Immunolabeling of antigens in plant cells. In Methods in Cell Biology, Vol. 37, Antibodies in Cell Biology, D.J. Asai, ed (San Diego: Academic Press), pp. 171–200.

Wilsbach, K., and Payne, G.S. (1993). Vps1p, a member of the dynamin GTPase family, is necessary for Golgi membrane protein retention in *Saccharomyces cerevisiae*. EMBO J. **12,** 3049–3059.

Zheng, H., von Mollard, G.F., Kovaleva, V., Stevens, T.H., and Raikhel, N.V. (1999). The plant vesicle-associated SNARE AtVTI1a likely mediates vesicle transport from the *trans*-Golgi network to the prevacuolar compartment. Mol. Biol. Cell **10,** 2251–2264.